Inorg. Chem. **2007**, *46*, 6452–6463

Occupation Waves the Way You Have Never Seen Them: the Orthorhombic Quasicrystal Approximants $RE_{13}Zn_{58+\delta}$ (RE = Ho, Er, Tm, and Lu)

ShuYing Piao* and Sven Lidin

Arrhenius Laboratory, Inorganic Chemistry, Stockholm University, S-106 91 Stockholm, Sweden

Received March 12, 2007

A series of binary quasicrystal approximants $RE_{13}Zn_{58+\delta}$ (RE = Ho, Er, Tm, and Lu) have been prepared, and structural studies were performed by means of single-crystal X-ray diffraction. All four compounds crystallize in the orthorhombic system, but while the Ho-containing compound crystallizes in space group *Pcmn*, the rest of the compounds crystallize in $Pc2_1n$. This work is a continuation of the structural studies on $RE_{13}Zn_{\sim 58}$ (RE = Ce, Pr, Nd, Sm, Gd, Tb, and Dy), which all belong to the hexagonal system. The sequence of $RE_{13}Zn_{58+\delta}$ compounds exhibits a large variability in local ordering and composition, and therefore the crystal structures are generally rather more complex than those previously reported and exhibit a number of different ordering modes. These four compounds are structurally closely related to each other.

Introduction

Studies of the structures of the 13:58 RE−Zn phases were first performed in 1967.[1,2] Soon afterward, such phases had been identified in a large number of rare/alkaline-earth Zn/Cd systems mainly by X-ray powder methods[3,4] but often without any structural details. The recent discovery of the first stable binary icosahedral quasicrystals in the Ca−Cd and Yb−Cd systems[5,6] has led to an intense study on the compositions, structures, and physical properties of such phases.[7−10] The structures of the quasicrystal approximants play a key role in understanding quasicrystals because they are expected to display the same local arrangement as those in the quasicrystals, with their long-range order making their structural determination possible by standard methods. Thus, the building blocks of quasicrystalline approximants contain high-symmetry polyhedra that can be used as possible models for components of quasicrystalline structures.[11−15]

A recent study capitalizes on these expected similarities to deliver the most detailed structural model of an icosahedral quasicrystal to date.[16]

This work, dealing with structures of the $RE_{13}Zn_{58+\delta}$ (RE = Ho, Er, Tm, and Lu) system, is a continuation of the structural studies on RE−Zn/Cd systems,[17−24] wherein the quasicrystal approximants have been shown to have rather more complex structures than those previously reported, and a number of different ordering modes have been identified. In fact, only the compounds $Ce_{13}Zn_{58}$ and $Pr_{13}Zn_{58}$ turn out

* To whom correspondence should be addressed. E-mail: sypiao@inorg.su.se.

(1) Larsson, A. C.; Cromer, D. T. *Acta Crystallogr.* **1967**, *23*, 70.
(2) Wang, F. E. *Acta Crystallogr.* **1967**, *22*, 579.
(3) Bruzzone, G.; Fornasini, M. L.; Merlo, F. *J. Less-Common Met.* **1970**, *22*, 253.
(4) Bruzzone, G.; Fornasini, M. L.; Merlo, F. *J. Less-Common Met.* **1974**, *37*, 289.
(5) Tsai, A. P.; Guo, J. Q.; Abe, E.; Takakura, H.; Sato, T. J. *Nature* **2000**, *408*, 537.
(6) Guo, J. Q.; Abe, E.; Tsai, A. P. *J. Phys. Rev. B* **2000**, *62*, R14605.
(7) Steurer, W. *Z. Kristallogr.* **1990**, *190*, 179.
(8) Yamamoto, A. *Acta Crystallogr., Sect. A* **1996**, *52*, 509.
(9) Tsai, A. P. *MRS Bull.* **1997**, *22*, 43.
(10) Maezawa, R.; Kashimoto, S.; Ishimasa, T. *Philos. Mag. Lett.* **2004**, *84*, 215.
(11) Bergman, G.; Waugh, J. L. T.; Pauling, L. *Nature* **1952**, *169*, 1057.
(12) Bergman, G.; Waugh, J. L. T.; Pauling, L. *Acta Crystallogr.* **1957**, *10*, 254.
(13) Cooper, M.; Robinson, K. *Acta Crystallogr.* **1966**, *20*, 614.
(14) Ishimasa, T.; Kaneko, Y.; Kaneko, H. *J. Non-Cryst. Solids* **2004**, *334*−*335*, 1.
(15) Ishimasa, T. In *The Science of Compex Alloy Phases*; Massalski, T. T., Turchi, P. E. A., Eds.; TMS (The Mineralogical Metals & Materials Society): Warrendale, PA, 2005; pp 231−249.
(16) Takakura, H.; Gómez, C. P.; Yamamoto, A.; Boissieu, M. D.; Tsai, A. P. *Nat. Mater.* **2006**, *6* (1), 58.
(17) Armbrüster, M.; Lidin, S. *J. Alloys Compd.* **2000**, *307*, 141.
(18) Gómez, C. P.; Lidin, S. *Angew. Chem.* **2001**, *113*, 21.
(19) Gómez, C. P.; Lidin, S. *Solid State Sci.* **2002**, *4*, 901.
(20) Gómez, C. P.; Lidin, S. *Phys. Rev. B: Condens. Matter Mater. Phys.* **2003**, *68*, 024203.
(21) Gómez, C. P.; Lidin, S. *Chem.—Eur. J.* **2004**, *10*, 3279.
(22) Piao, S.; Gómez, C. P.; Lidin, S. *Z. Naturforsch.* **2006**, *60b*, 644.
(23) Piao, S. Y.; Gómez, C. P.; Lidin, S. *Z. Kristallogr.* **2006**, *221*, 391.
(24) Piao, S. Y.; Lidin, S. *Philos. Mag.* **2007**, *87*, 2693.

10.1021/ic700476w CCC: $37.00
Published on Web 07/10/2007

Table 1. Experimental Details for the Syntheses of $RE_{13}Zn_{58+\delta}$

RE	amount of *RE* metals (g)	amount of Zn metals (g)	material atomic *RE*:Zn	annealing temp (K)	annealing time (h)	main product *RE*:Zn	comment
Ho	0.3612	0.6498	13:58	1143	90	1:3	
	0.1717	0.3945	13:75	1113	72	3:22	
	0.3612	0.4916	13:44	1113	120	13:58	powder product
	0.1717	0.3945	13:75	1113	72	3:22	
	0.4543	0.6156	13:44	1113	120	13:58	powder product
	0.3428	0.4665	13:44	1113	48	13:58	ref 24
	0.2553	*0.5425*	*13:69*	*1108*	*96*	*13:58*	*used in this paper*
Er	0.3425	0.5875	13:58	1123	48	3:11	
	0.3568	0.5875	13:58	1108	120	1:3	
	0.3389	0.6787	13:67	1108	48	2:17	
	0.3644	*0.6356*	*13:58*	*1143*	*96*	*13:58*	*used in this paper*
Tm	0.3667	0.6333	13:58	1113	96	1:5	
	0.3764	*0.6501*	*13:58*	*1108*	*96*	*13:58*	*used in this paper*
Lu	*0.1503*	*0.3505*	*13:81*	*1108*	*96*	*13:58*	*used in this paper*

Table 2. Comparison of the Compositions of the Compounds from EDX Analyses and Refinements

compound	$Ho_{13}Zn_{58.71}$	$Er_{12.89}Zn_{58.82}$	$Tm_{12.88}Zn_{58.64}$	$Lu_{12.71}Zn_{58.54}$
normalized ratio of *RE*:Zn (from EDX analysis)	13:63(1)	12.89:58.7(5)	12.88:58.6(2)	12.7:58.5(2)
ratio of *RE*:Zn (from refinement)	13:58.71(1)	12.89:58.82(1)	12.88:58.64(1)	12.71:58.54(1)

Table 3. Crystal Data, Data Collection, and Refinement Parameters for the Structures

formula	$Ho_{13}Zn_{58.71}$	$Er_{12.89}Zn_{58..82}$	$Tm_{12.88}Zn_{58.64}$	$Lu_{12.71}Zn_{58.54}$
molar mass (g mol^{-1})	5982.6	6000.9	6009.7	6051.3
temp of measurement (K)	293	293	293	293
space group	*Pcmn*	*Pc*2$_1$*n*	*Pc*2$_1$*n*	*Pc*2$_1$*n*
a (Å)	24.625(1)	24.695(1)	24.515 (1)	24.428(1)
b (Å)	14.245(1)	14.247(1)	14.165(1)	14.112(1)
c (Å)	14.007(1)	14.045(1)	13.948(1)	13.919(1)
cell volume (Å^3)	4913.6(4)	4941.4(4)	4843.6(4)	4798.1(4)
Z	4	4	4	4
F(000)	10 534	10 563	10 592	10 638
calcd density (g cm^{-3})	8.085	8.064	8.239	8.374
abs coeff	48.64	49.49	51.58	54.45
range of 2θ (deg)	9.1−53.4	11.3 − 55.2	11.6−55.4	9.3 − 54.5
obsd reflns [$I > 3\sigma(I)$]	7356	15 438	11 320	10 466
indep reflns	5484	8988	6378	6453
no. of param	366	380	355	324
anisotropic param applied to	Ho and Zn atoms	Er atoms	part of the Tm atoms	none
R_{int} (obs/all)	7.88/8.11	6.44/7.00	5.57/5.95	6.41/6.63
R_1 (obs/all)	4.99/7.27	4.96/8.06	5.50/8.50	5.01/7.33
R_w (obs/all)	4.93/5.52	5.18/5.32	5.34/5.71	5.03/5.32
abs corrn	numerical, from shape	numerical, from shape	numerical, from shape	numerical, from shape
T_{min}, T_{max}	0.0124, 0.0538	0.0978, 0.5834	0.0098, 0.584	0.0434, 0.2076
$\Delta\rho_{max}$, $\Delta\rho_{min}$ (e Å^{-3})	4.43, −5.78	5.72, −4.94	3.89, −3.02	4.73, −5.22

to adhere to the archetype structure reported long time ago. In the Nd compound, a disorder mechanism (disorder mechanism I) is present whereby the *RE* position on the hexad (*RE*4) is partially replaced by a Zn_2 dumbbell (Zn13). For Sm and Gd, which both display disorder mechanism I, an additional partially occupied position (Zn14) breaks the centrosymmetry of the structures, reducing the symmetry to $P6_3mc$ (disorder mechanism II). For the Tb structure, disorder mechanism I is absent while disorder mechanism II orders to produce an orthorhombic superstructure, and for the Dy structure, disorder mechanism I is present and yet a third phenomenon is exhibited. There is only one Zn atom in the archetype structure that has no short contacts to any rare-earth atom, and this is Zn12. This atom resides in a perfect Zn_8 cube. In the Dy compound, the structure becomes orthorhombic as a result of ordered vacancies on these positions in cubic interstices. This behavior is reminiscent of the structuring in the cubic $RECd_6$ compounds, where similar cubic interstices are subject to partial occupancy that interacts in a complex manner with surrounding disordered entities. All compounds covered in this study represent new, closely related, types.

Experimental Section

Synthesis. Chips of rare-earth metal (STREM and CHEMPUR 99.9%) and Zn ingot (Baker Chemicals 99.9%) were mixed in niobium ampules in stoichiometric proportions. For the Lu compound, a slightly more rare-earth-metal-rich mixture proved optimal. The ampules were sealed under an argon atmosphere. Several different annealing temperatures and compositions were tried to optimize the yield of the target phase. At first, a stoichiometric composition for $RE_{13}Zn_{58}$ was tried at different annealing temperatures from 800 K up to 1200 K. If the target phase was not obtained by this procedure, then the composition was shifted to either the rare-earth-metal-rich side or the Zn-rich side according to the phase produced by previous procedures. In order to obtain the desired phase in a well-crystallized state, it was found to be effective to anneal the ampules for a period of 48−96 h at about 20 K below the reported melting points for each phase. Reaction times did not

Table 4. Fractional Atomic Coordinates, Occupancies, and Isotropic ADPs for the $Ho_{13}Zn_{58.71}$ Compound

element	atom	Wyckoff	occu. ≠ 1	*x*	*y*	*z*	U_{iso}/U_{eq} (Å^2)
Ho	Ho1a	8d		−0.01997(4)	0.43446(7)	−0.25611(7)	0.0074(3)
Ho	Ho1b	4c		0.29365(6)	−1/4	−0.25761(10)	0.0076(4)
Ho	Ho2a	8d		0.14717(4)	−0.06273(7)	−0.05339(7)	0.0086(3)
Ho	Ho2b	8d		0.64687(4)	0.44157(7)	−0.05326(7)	0.0066(3)
Ho	Ho2c	4c		0.45436(6)	1/4	−0.05142(10)	0.0063(4)
Ho	Ho2d	4c		0.95317(6)	3/4	−0.05691(10)	0.0068(4)
Ho	Ho3a	8d		−0.18629(4)	−0.05798(7)	−0.26829(8)	0.0180(4)
Ho	Ho3b	4c		0.62743(6)	−1/4	−0.2089(1)	0.0078(4)
Ho	Ho4	4c		0.24267(6)	1/4	−0.00713(12)	0.0151(4)
Zn	Zn1a	8d		0.56663(10)	0.90076(18)	−0.09785(18)	0.0092(8)
Zn	Zn1b	8d		0.26772(10)	−0.11207(18)	−0.09929(18)	0.0096(8)
Zn	Zn1c	8d		0.76825(10)	0.4175(2)	−0.10322(19)	0.0194(9)
Zn	Zn1d	8d		0.07378(12)	0.4607(2)	0.0977(2)	0.0262(10)
Zn	Zn1e	8d		0.5855(1)	0.95028(18)	0.09931(18)	0.0106(8)
Zn	Zn1l	8d	0.5	0.9357(3)	0.5911(5)	0.0924(5)	0.0155(12)
Zn	Zn2a	4c		0.08097(14)	3/4	−0.0956(2)	0.0086(10)
Zn	Zn2b	4c		0.58396(14)	1/4	−0.0950(2)	0.0068(10)
Zn	Zn3	4c		0.08216(16)	3/4	−0.7497(3)	0.0141(11)
Zn	Zn4a	8d		0.19617(11)	0.1076(2)	−0.1661(2)	0.0202(9)
Zn	Zn4b	8d		0.71443(11)	0.6027(2)	−0.14700(18)	0.0160(8)
Zn	Zn4c	4c		0.34367(15)	1/4	−0.1499(3)	0.0142(12)
Zn	Zn4d	4c		0.84444(15)	3/4	−0.1677(2)	0.0107(11)
Zn	Zn5a	8d		0.16174(16)	0.3881(3)	0.0552(3)	0.0569(15)
Zn	Zn5b	8d		0.65249(10)	0.84786(19)	−0.00449(19)	0.0099(7)
Zn	Zn5c	8d		0.25604(11)	0.04821(18)	−0.0265(2)	0.0154(8)
Zn	Zn6a	8d		0.20789(10)	−0.07465(19)	−0.24824(18)	0.0114(8)
Zn	Zn6b	8d		0.43170(11)	0.35235(19)	−0.25015(18)	0.0121(8)
Zn	Zn6c	8d		0.39251(10)	0.4722(2)	0.25300(19)	0.0133(8)
Zn	Zn7a	8d		0.02941(11)	−0.4076(2)	−0.13922(18)	0.0154(8)
Zn	Zn7b	8d		0.53095(10)	0.09516(18)	−0.14203(17)	0.0105(8)
Zn	Zn7c	4c		0.68647(14)	1/4	−0.1454(3)	0.0116(11)
Zn	Zn7d	4c		0.18857(14)	3/4	−0.1427(3)	0.0098(11)
Zn	Zn8a	8d		−0.04715(11)	0.3520(2)	−0.05234(19)	0.0193(9)
Zn	Zn8b	8d		0.45007(10)	0.84760(18)	−0.04947(17)	0.0096(8)
Zn	Zn8c	4c		0.34524(14)	−1/4	−0.0480(3)	0.0093(11)
Zn	Zn8d	4c		0.85813(15)	1/4	−0.0553(3)	0.0119(11)
Zn	Zn9a	8d		−0.13108(10)	0.09957(19)	−0.15891(17)	0.0109(8)
Zn	Zn9b	8d		0.36914(10)	0.60872(18)	−0.15682(16)	0.0075(7)
Zn	Zn9c	4c		0.51317(13)	−1/4	−0.1578(3)	0.0085(11)
Zn	Zn9d	4c		0.02114(14)	1/4	−0.1571(3)	0.0110(11)
Zn	Zn10a	8d		0.11409(10)	−0.15340(17)	−0.24890(18)	0.0083(7)
Zn	Zn10b	4c		0.48189(14)	3/4	0.2502(3)	0.0099(11)
Zn	Zn11	4c		0.25000(16)	1/4	−0.2473(3)	0.0125(10)
Zn	Zn12a	4b		1/2	0	0.00000	0.0127(11)
Zn	Zn12b	4c		0.24299(15)	3/4	0.0176(3)	0.0235(14)
Zn	Zn14	4c	0.378(16)	0.8684(5)	3/4	0.0877(8)	0.0155(12)
Zn	ZnX1	8d	0.184(6)	0.9906(6)	0.5225(10)	0.0179(10)	0.0155(12)
Zn	ZnX2	8d	0.306(7)	0.9624(4)	0.5605(7)	0.0647(7)	0.0155(12)
Zn	ZnX3	8d	0.213(9)	0.9170(6)	0.6199(11)	0.1091(10)	0.0155(12)
Zn	ZnX4	8d	0.283(9)	0.8796(4)	0.6585(10)	0.0876(7)	0.0155(12)
Zn	ZnX5	8d	0.183(8)	0.8668(8)	0.704(2)	0.0830(12)	0.0155(12)

prove crucial for crystal quality. The furnaces were then turned off with the samples left inside to cool down to ambient temperature (cooling rate 1−3 °C min^{-1}). Normally, single crystals would only form for the majority phase in each batch. All products were silvery and brittle, with irregular shapes. Single crystals could easily be isolated from the resulting samples. All preparations were carried out in an inert atmosphere (argon) in order to avoid detrimental effects from water vapor or oxygen. All pertinent details of the experiments are given in Table 1.

Scanning Electron Microscopy and Energy-Dispersive X-ray Analysis. Elemental analysis on single crystals was performed with a JEOL JSM-820 scanning electron microscope equipped with a Link EDX (energy-dispersive X-ray) analysis system operated at 20 kV. Corrections were made for atomic number, absorption, and fluorescence. EDX analysis was performed on approximately six different crystals from each synthesized sample in order to ascertain the elemental purity but not on the crystals used for diffraction experiments because they were encapsulated in droplets of epoxy glue to protect them from the surrounding atmosphere. The analyses were generally in good agreement with the final compositions obtained from the refinements, as shown in Table 2. In all reactions, the target structures were the major crystalline products.

Single-Crystal X-ray Data Collection and Structural Refinement. For the diffraction experiments, several crystals from each batch were selected from the crushed sample and mounted on a glass fiber. The crystal habit was irregular. The crystals on which the final measurements were performed were selected to be free of parasites. Single-crystal X-ray diffraction data collection was performed for detailed structural analyses at ambient temperature on an Oxford Diffraction Xcalibur CCD diffractometer with graphite-monochromatized Mo Kα radiation (λ = 0.710 73 Å), operated at 50 kV and 40 mA, and a detector-to-crystal distance of 80 mm. The intensities of the reflections were integrated using the software supplied by the manufacturers of the diffractometer.[25,26] Because of the irregular shape of the crystals and twinning, absorption correction on such a crystal by the actual measurement of the shape is inapplicable. Therefore, a numerical absorption

(25) Oxford Diffraction. *CrysAlis CCD*; 2006; p 171.31.2.
(26) Oxford Diffraction. *CrysAlis RED*; 2006; p 171.31.2.

Table 5. Fractional Atomic Coordinates, Occupancies, and Isotropic ADPs for the $Er_{12.89}Zn_{58.82}$ Compound

element	atom	Wyckoff	occu. ≠ 1	*x*	*y*	*z*	U_{iso}/U_{eq} (Å^2)
Er	Er1a	4a		−0.01992(13)	0.4345(4)	−0.2542(5)	0.0108(10)
Er	Er1b	4a		0.02069(13)	−0.4346(4)	0.2560(4)	0.0076(10)
Er	Er1c	4a		0.29385(6)	−0.2486(5)	−0.2568(3)	0.0083(5)
Er	Er2a	4a		0.14744(16)	−0.06159	−0.0535(3)	0.0113(14)
Er	Er2b	4a		−0.14717(15)	0.0638(3)	0.0535(3)	0.0086(13)
Er	Er2c	4a		0.64662(15)	0.4417(5)	−0.0525(3)	0.0076(13)
Er	Er2d	4a		−0.64683(15)	−0.4406(5)	0.0528(3)	0.0083(13)
Er	Er2e	4a		0.45484(10)	0.2512(6)	−0.0510(2)	0.0081(8)
Er	Er2f	4a		0.95364(10)	0.7514(6)	−0.0568(2)	0.0075(8)
Er	Er3a	4a		−0.18665(16)	−0.0580(4)	−0.2682(4)	0.0156(16)
Er	Er3b	4a		0.18598(16)	0.0592(4)	0.2682(4)	0.0175(16)
Er	Er3c	4a		0.62733(7)	−0.2493(5)	−0.21033(11)	0.0119(5)
Er	Er4	4a	0.887(4)	0.24299(11)	0.2512(5)	−0.0055(3)	0.0170(7)
Zn	Zn1a	4a		0.5689(4)	0.8959(7)	−0.1006(7)	0.012(2)
Zn	Zn1b	4a		−0.5638(3)	−0.9057(6)	0.0963(5)	−0.0041(17)
Zn	Zn1c	4a		0.2682(3)	−0.1175(7)	−0.0983(6)	0.010(2)
Zn	Zn1d	4a		−0.2678(3)	0.1066(7)	0.0989(6)	−0.0011(17)
Zn	Zn1e	4a		0.7673(4)	0.4132(7)	−0.1014(6)	0.010(2)
Zn	Zn1f	4a		−0.7691(3)	−0.4270(7)	0.1076(6)	0.016(2)
Zn	Zn1g	4a		0.0679(3)	0.4640(6)	0.0868(6)	0.0165(18)
Zn	Zn1h	4a		−0.0791(4)	−0.4569(8)	−0.1049(7)	0.022(2)
Zn	Zn1i	4a		0.5877(3)	0.9477(6)	0.1028(6)	0.0011(18)
Zn	Zn1j	4a		−0.5843(4)	−0.9514(9)	−0.0964(8)	0.016(3)
Zn	Zn1k	4a	0.620(27)	0.9260(6)	0.6047(11)	0.1017(10)	0.0165(16)
Zn	Zn1l	4a	0.650(27)	−0.9377(6)	−0.5905(10)	−0.0883(9)	0.0165(16)
Zn	Zn2a	4a		0.0812(2)	0.748(1)	−0.0936(4)	0.0066(14)
Zn	Zn2b	4a		0.5839(2)	0.2535(10)	−0.0965(4)	0.0072(15)
Zn	Zn3	4a		0.08199(16)	0.7482(7)	−0.7572(4)	0.0099(6)
Zn	Zn4a	4a		0.1971(3)	0.1034(6)	−0.1687(5)	0.0064(16)
Zn	Zn4b	4a		−0.1930(4)	−0.1123(8)	0.1585(7)	0.022(2)
Zn	Zn4c	4a		0.7163(3)	0.6030(7)	−0.1430(7)	0.022(2)
Zn	Zn4d	4a		−0.7109(4)	−0.5995(7)	0.1536(7)	0.012(2)
Zn	Zn4e	4a		0.3444(2)	0.2447(9)	−0.1510(5)	0.0165(16)
Zn	Zn4f	4a		0.8458(2)	0.7567(9)	−0.1663(4)	0.0115(15)
Zn	Zn5a	4a		0.1656(3)	0.3966(6)	0.0648(5)	0.0258(16)
Zn	Zn5b	4a		−0.1564(3)	−0.3729(6)	−0.0388(6)	0.0276(19)
Zn	Zn5c	4a		0.6530(4)	0.8494(7)	−0.0035(7)	0.0049(19)
Zn	Zn5d	4a		−0.6537(4)	−0.8455(8)	0.0052(8)	0.012(2)
Zn	Zn5e	4a		0.2542(5)	0.0503(7)	−0.0204(7)	0.018(2)
Zn	Zn5f	4a		−0.2582(4)	−0.0482(6)	0.0290(6)	0.0082(19)
Zn	Zn6a	4a		0.2079(2)	−0.0670(5)	−0.2454(9)	0.0111(17)
Zn	Zn6b	4a		−0.2076(2)	0.0812(5)	0.2517(10)	0.0064(14)
Zn	Zn6c	4a		0.4327(3)	0.3528(6)	−0.2537(9)	0.0104(18)
Zn	Zn6d	4a		−0.4318(3)	−0.3510(6)	0.2456(9)	0.0123(19)
Zn	Zn6e	4a		0.3933(3)	0.4753(6)	0.2548(11)	0.0111(19)
Zn	Zn6f	4a		−0.3919(3)	−0.4700(6)	−0.2506(12)	0.0116(18)
Zn	Zn7a	4a		0.0288(4)	−0.4032(7)	−0.1457(6)	0.009(2)
Zn	Zn7b	4a		−0.0310(3)	0.4119(7)	0.1308(5)	0.0106(19)
Zn	Zn7c	4a		0.5307(4)	0.0930(9)	−0.1415(8)	0.009(2)
Zn	Zn7d	4a		−0.5310(4)	−0.0962(9)	0.1443(8)	0.015(3)
Zn	Zn7e	4a		0.6870(3)	0.2585(7)	−0.1459(5)	0.0105(17)
Zn	Zn7f	4a		0.1883(2)	0.7468(8)	−0.1425(4)	0.0053(14)
Zn	Zn8a	4a		−0.0453(3)	0.3607(7)	−0.0494(5)	0.0098(18)
Zn	Zn8b	4a		0.0494(4)	−0.3431(8)	0.0546(7)	0.017(2)
Zn	Zn8c	4a		0.4484(3)	0.8420(6)	−0.0515(5)	0.0004(15)
Zn	Zn8d	4a		−0.4518(4)	−0.8535(7)	0.0492(7)	0.012(2)
Zn	Zn8e	4a		0.3454(2)	−0.2478(11)	−0.0483(4)	0.0055(11)
Zn	Zn8f	4a		0.8587(2)	0.2492(11)	−0.0563(4)	0.0161(14)
Zn	Zn9a	4a		−0.1317(5)	0.1008(10)	−0.1575(10)	0.009(3)
Zn	Zn9b	4a		0.1303(5)	−0.096(1)	0.1602(10)	0.011(3)
Zn	Zn9c	4a		0.3688(5)	0.6112(9)	−0.1578(10)	0.008(3)
Zn	Zn9d	4a		−0.3692(4)	−0.6068(9)	0.1578(10)	0.005(3)
Zn	Zn9e	4a		0.5133(2)	−0.2448(9)	−0.1573(4)	0.0041(13)
Zn	Zn9f	4a		0.0214(2)	0.2483(10)	−0.1569(4)	0.0130(15)
Zn	Zn10a	4a		0.1135(3)	−0.1531(6)	−0.2500(14)	0.0109(18)
Zn	Zn10b	4a		−0.1147(3)	0.1549(6)	0.2503(13)	0.0075(17)
Zn	Zn10c	4a		0.48176(13)	0.7555(7)	0.2499(6)	0.0062(8)
Zn	Zn11	4a		0.24994(16)	0.2500(8)	−0.2392(3)	0.0123(6)
Zn	Zn12a	4a		0.4980(5)	0.0017(9)	−0.0024(9)	0.0114(10)
Zn	Zn12b	4a		0.24226(18)	0.7422(6)	0.0168(3)	0.0155(13)
Zn	Zn13a	4a	0.113(4)	0.2452(17)	0.263(4)	0.091(3)	0.002(6)
Zn	Zn13b	4a	0.113(4)	0.2445(17)	0.262(4)	−0.088(4)	0.002(6)
Zn	Zn14	4a	0.606(14)	0.8682(3)	0.7664(8)	0.0872(5)	0.0162(16)
Zn	Znx1	4a	0.386(16)	0.9841(6)	0.5253(13)	0.0134(14)	0.0162(16)
Zn	Znx2	4a	0.440(23)	0.9596(8)	0.5700(13)	0.0736(13)	0.0162(16)
Zn	Znx3	4a	0.443(15)	0.8785(5)	0.6654(9)	0.0864(9)	0.0162(16)
Zn	Znx4	4a	0.220(22)	0.9685(12)	0.9549(2)	0.0490(2)	0.0162(16)
Zn	Znx5	4a	0.218(17)	0.9066(13)	0.8650(2)	0.1111(19)	0.0162(16)

Table 6. Fractional Atomic Coordinates, Occupancies, and Isotropic ADPs for the $Tm_{12.88}Zn_{58.64}$ Compound

element	atom	Wyckoff	occu. ≠ 1	*x*	*y*	*z*	U_{iso}/U_{eq} (Å^2)
Tm	Tm1a	4a		−0.02007(14)	0.4345(3)	−0.25584(19)	0.0076(10)
Tm	Tm1b	4a		0.02044(14)	−0.4343(3)	0.2550(2)	0.0103(11)
Tm	Tm1c	4a		0.29438(5)	−0.2494(4)	−0.25767(9)	0.0087(3)
Tm	Tm2a	4a		0.14751(13)	−0.06311	−0.0535(2)	0.0095(7)
Tm	Tm2b	4a		−0.14762(13)	0.06487(12)	0.0534(2)	0.0091(8)
Tm	Tm2c	4a		0.64641(13)	0.4423(3)	−0.0525(2)	0.0081(7)
Tm	Tm2d	4a		−0.64695(13)	−0.4400(3)	0.0532(2)	0.0080(7)
Tm	Tm2e	4a		0.45474(5)	0.2512(4)	−0.05153(8)	0.0089(3)
Tm	Tm2f	4a		0.95360(5)	0.7509(4)	−0.05739(8)	0.0082(3)
Tm	Tm3a	4a		−0.18693(15)	−0.0582(4)	−0.2685(3)	0.0158(11)
Tm	Tm3b	4a		0.18643(15)	0.0595(4)	0.2677(3)	0.0185(11)
Tm	Tm3c	4a		0.62743(5)	−0.2499(4)	−0.20901(9)	0.0125(4)
Tm	Tm4	4a	0.880(4)	0.24266(6)	0.2500(5)	−0.00382(12)	0.0172(5)
Zn	Zn1a	4a		0.5676(3)	0.9013(6)	−0.0988(6)	0.0107(19)
Zn	Zn1b	4a		−0.5653(3)	−0.8998(6)	0.0976(6)	0.0116(19)
Zn	Zn1c	4a		0.2674(4)	−0.1116(7)	−0.0986(6)	0.017(2)
Zn	Zn1d	4a		−0.2682(3)	0.1109(6)	0.0994(6)	0.0081(17)
Zn	Zn1e	4a		0.7686(4)	0.4230(6)	−0.1046(6)	0.018(2)
Zn	Zn1f	4a		−0.7675(4)	−0.4133(6)	0.1025(6)	0.017(2)
Zn	Zn1g	4a		0.0654(2)	0.4673(5)	0.0848(4)	0.0123(13)
Zn	Zn1h	4a		−0.0771(3)	−0.4557(5)	−0.1006(4)	0.0280(18)
Zn	Zn1i	4a		0.5844(3)	0.9517(6)	0.0997(6)	0.0124(19)
Zn	Zn1j	4a		−0.5871(3)	−0.9482(6)	−0.1000(5)	0.0123(19)
Zn	Zn1k	4a	0.710(22)	0.9347(5)	0.5923(8)	0.0906(7)	0.0148(12)
Zn	Zn1l	4a	0.384(17)	−0.9557(8)	−0.5701(12)	−0.0756(11)	0.0148(12)
Zn	Zn2	4a		0.08179(13)	0.7508(11)	−0.7514(2)	0.0141(6)
Zn	Zn3a	4a		0.08111(13)	0.7505(9)	−0.0952(2)	0.0078(6)
Zn	Zn3b	4a		0.58378(13)	0.2495(9)	−0.0950(2)	0.0101(7)
Zn	Zn4a	4a		0.1929(3)	0.1115(6)	−0.1596(5)	0.0130(17)
Zn	Zn4b	4a		−0.1968(4)	−0.1051(7)	0.1667(6)	0.028(2)
Zn	Zn4c	4a		0.7099(3)	0.5981(6)	−0.1531(5)	0.0187(19)
Zn	Zn4d	4a		−0.7158(3)	−0.6025(6)	0.1459(5)	0.0179(19)
Zn	Zn4e	4a		0.34466(13)	0.2516(9)	−0.1505(2)	0.0159(8)
Zn	Zn4f	4a		0.84579(13)	0.7499(9)	−0.1671(2)	0.0126(7)
Zn	Zn5a	4a		0.1649(3)	0.3964(5)	0.0630(5)	0.0360(18)
Zn	Zn5b	4a		−0.1554(3)	−0.3784(5)	−0.0418(5)	0.0318(17)
Zn	Zn5c	4a		0.6526(3)	0.8492(7)	−0.0024(6)	0.0127(19)
Zn	Zn5d	4a		−0.6532(3)	−0.8460(6)	0.0066(6)	0.0110(18)
Zn	Zn5e	4a		0.2555(3)	0.0499(7)	−0.0241(7)	0.017(2)
Zn	Zn5f	4a		−0.2564(3)	−0.0501(7)	0.0277(7)	0.020(2)
Zn	Zn6a	4a		0.2077(3)	−0.0726(7)	−0.2479(5)	0.009(2)
Zn	Zn6b	4a		−0.2080(4)	0.0763(8)	0.2489(6)	0.016(2)
Zn	Zn6c	4a		0.4320(4)	0.3547(8)	−0.2529(5)	0.015(2)
Zn	Zn6d	4a		−0.4316(4)	−0.3516(8)	0.2510(5)	0.013(2)
Zn	Zn6e	4a		0.3920(3)	0.4718(7)	0.2531(5)	0.008(2)
Zn	Zn6f	4a		−0.3935(4)	−0.4733(8)	−0.2535(6)	0.020(3)
Zn	Zn7a	4a		0.0295(3)	−0.4076(6)	−0.1412(6)	0.0134(19)
Zn	Zn7b	4a		−0.0299(3)	0.4123(6)	0.1336(6)	0.016(2)
Zn	Zn7c	4a		0.5308(4)	0.0953(7)	−0.1423(6)	0.012(2)
Zn	Zn7d	4a		−0.5307(4)	−0.0935(7)	0.1434(6)	0.013(2)
Zn	Zn7e	4a		0.68680(13)	0.2524(9)	−0.1455(2)	0.0128(7)
Zn	Zn7f	4a		0.18914(13)	0.7491(9)	−0.1441(2)	0.0098(7)
Zn	Zn8a	4a		−0.0434(3)	0.3611(6)	−0.0495(5)	0.0165(19)
Zn	Zn8b	4a		0.0481(3)	−0.3485(5)	0.0531(5)	0.0130(17)
Zn	Zn8c	4a		0.4503(4)	0.8469(6)	−0.0498(5)	0.0088(19)
Zn	Zn8d	4a		−0.4496(4)	−0.8479(6)	0.0511(6)	0.013(2)
Zn	Zn8e	4a		0.34528(12)	−0.2490(8)	−0.0493(2)	0.0082(7)
Zn	Zn8f	4a		0.85898(13)	0.2516(9)	−0.0563(2)	0.0159(8)
Zn	Zn9a	4a		−0.1308(4)	0.0978(7)	−0.1578(6)	0.016(2)
Zn	Zn9b	4a		0.1303(3)	−0.0980(6)	0.1584(6)	0.0088(18)
Zn	Zn9c	4a		0.3691(4)	0.6076(7)	−0.1574(6)	0.0099(18)
Zn	Zn9d	4a		−0.3694(3)	−0.6084(6)	0.1578(6)	0.0078(18)
Zn	Zn9e	4a		0.51332(12)	−0.2500(9)	−0.1583(2)	0.0086(7)
Zn	Zn9f	4a		0.02172(13)	0.2501(9)	−0.1568(2)	0.0108(7)
Zn	Zn10a	4a		0.1139(4)	−0.1531(8)	−0.2484(6)	0.013(2)
Zn	Zn10b	4a		−0.1142(4)	0.1543(7)	0.2506(5)	0.008(2)
Zn	Zn10c	4a		0.48173(11)	0.7495(10)	0.2506(2)	0.0085(6)
Zn	Zn11	4a		0.24964(13)	0.2493(9)	−0.2482(3)	0.0216(10)
Zn	Zn12a	4a		0.5012(5)	0.0023(9)	0.0008(9)	0.0182(8)
Zn	Zn12b	4a		0.24196(14)	0.7427(6)	0.0165(2)	0.0199(10)
Zn	Zn13a	4a	0.120(17)	0.2540(11)	0.257(4)	0.0874(17)	0.007(6)
Zn	Zn13b	4a	0.120(4)	0.2550(11)	0.262(3)	−0.0877(18)	0.007(6)
Zn	Zn14	4a	0.637(11)	0.8687(2)	0.7604(8)	0.0855(4)	0.0148(12)
Zn	ZnX1	4a	0.175(11)	0.9835(9)	0.9841(19)	0.0074(19)	0.0148(12)
Zn	ZnX2	4a	0.620(24)	0.9293(5)	0.8996(9)	0.0983(8)	0.0148(12)
Zn	ZnX3	4a	0.210(13)	0.9011(11)	0.8576(18)	0.1062(16)	0.0148(12)
Zn	ZnX4	4a	0.291(16)	0.9689(8)	−0.4459(13)	0.0514(14)	0.0148(12)
Zn	ZnX5	4a	0.366(13)	0.8768 (6)	0.665(1)	0.0839(9)	0.0148(12)

Table 7. Fractional Atomic Coordinates, Occupancies, and Isotropic ADPs for the $Lu_{12.71}Zn_{58.54}$ Compound

element	atom	Wyckoff	occu. ≠ 1	*x*	*y*	*z*	U_{iso}/U_{eq} (Å^2)
Lu	Lu1a	4a		−0.0210(2)	0.4356(4)	−0.2541(3)	0.0090(9)
Lu	Lu1b	4a		0.0205(2)	−0.4331(4)	0.2532(3)	0.0089(9)
Lu	Lu1c	4a		0.29425(11)	−0.2502(5)	−0.25704(13)	0.0080(5)
Lu	Lu2a	4a		0.14779(17)	−0.06251	−0.0531(3)	0.0089(9)
Lu	Lu2b	4a		−0.14718(17)	0.06415(19)	0.0533(3)	0.0090(9)
Lu	Lu2c	4a		0.64640(17)	0.4413(3)	−0.0521(3)	0.0080(8)
Lu	Lu2d	4a		−0.64684(17)	−0.4401(3)	0.0526(3)	0.0062(8)
Lu	Lu2e	4a		0.45586(9)	0.2508(4)	−0.05083(14)	0.0086(5)
Lu	Lu2f	4a		0.95477(9)	0.7505(4)	−0.05646(13)	0.0083(5)
Lu	Lu3a	4a		−0.1870(2)	−0.0592(4)	−0.2685(3)	0.0169(11)
Lu	Lu3b	4a		0.1868(2)	0.0610(4)	0.2655(4)	0.0236(13)
Lu	Lu3c	4a		0.62650(9)	−0.2499(5)	−0.21172(15)	0.0160(5)
Lu	Lu4	4a	0.713(4)	0.24494(11)	0.2497(6)	0.0002(2)	0.0138(5)
Zn	Zn1a	4a		0.5682(4)	0.8991(7)	−0.0989(7)	0.006(2)
Zn	Zn1b	4a		−0.5632(4)	−0.9022(7)	0.0973(7)	0.010(2)
Zn	Zn1c	4a		0.2676(4)	−0.1052(7)	−0.0992(8)	0.009(2)
Zn	Zn1d	4a		−0.2678(5)	0.1154(8)	0.0966(8)	0.019(3)
Zn	Zn1e	4a		0.7688(4)	0.4288(7)	−0.1057(7)	0.017(2)
Zn	Zn1f	4a		−0.7666(4)	−0.4096(7)	0.1003(7)	0.012(2)
Zn	Zn1g	4a		0.0661(3)	0.4651(6)	0.0874(6)	0.017(2)
Zn	Zn1h	4a		−0.0795(5)	−0.4513(9)	−0.0996(9)	0.049(4)
Zn	Zn1i	4a		0.5862(4)	0.9520(7)	0.1003(7)	0.004(2)
Zn	Zn1j	4a		−0.5857(5)	−0.9465(8)	−0.1003(9)	0.022(3)
Zn	Zn1k	4a	0.730(25)	−0.9411(5)	−0.5898(8)	−0.0909(8)	0.0042(14)
Zn	Zn1l	4a	0.600(25)	0.9285(6)	0.6018(10)	0.0959(9)	0.0042(14)
Zn	Zn2a	4a		0.0820(2)	0.7521(9)	−0.0948(3)	0.0070(9)
Zn	Zn2b	4a		0.5846(3)	0.2533(9)	−0.0949(3)	0.0094(9)
Zn	Zn3	4a		0.0832(4)	0.7525(11)	−0.7524(4)	0.0121(5)
Zn	Zn4a	4a		0.1935(4)	0.1121(7)	−0.1587(8)	0.013(2)
Zn	Zn4b	4a		−0.1941(5)	−0.1049(8)	0.1629(8)	0.018(3)
Zn	Zn4c	4a		0.7109(4)	0.5974(8)	−0.1511(8)	0.014(3)
Zn	Zn4d	4a		−0.7083(5)	−0.5964(9)	0.1541(9)	0.024(3)
Zn	Zn4e	4a		0.3461(3)	0.2540(11)	−0.1514(5)	0.0254(16)
Zn	Zn4f	4a		0.8468(2)	0.7532(10)	−0.1669(4)	0.0188(15)
Zn	Zn5a	4a		0.1582(5)	0.3747(8)	0.0377(8)	0.042(3)
Zn	Zn5b	4a		−0.1620(4)	−0.3913(7)	−0.0599(7)	0.041(3)
Zn	Zn5c	4a		0.6532(5)	0.8477(8)	−0.0022(8)	0.018(3)
Zn	Zn5d	4a		−0.6520(4)	−0.8464(8)	0.0072(7)	0.009(2)
Zn	Zn5e	4a		0.2545(4)	0.0569(8)	−0.0187(8)	0.019(3)
Zn	Zn5f	4a		−0.2578(4)	−0.0492(8)	0.0275(8)	0.016(2)
Zn	Zn6a	4a		0.2086(5)	−0.0751(9)	−0.2486(8)	0.014(3)
Zn	Zn6b	4a		−0.2082(5)	0.0767(9)	0.2491(8)	0.008(3)
Zn	Zn6c	4a		0.4326(5)	0.3519(8)	−0.2515(8)	0.011(3)
Zn	Zn6d	4a		−0.4316(5)	−0.3540(9)	0.2516(8)	0.017(3)
Zn	Zn6e	4a		0.3920(5)	0.4714(8)	0.2523(8)	0.011(3)
Zn	Zn6f	4a		−0.3918(5)	−0.4737(9)	−0.2527(9)	0.018(3)
Zn	Zn7a	4a		0.0305(4)	−0.4103(8)	−0.1374(7)	0.011(2)
Zn	Zn7b	4a		−0.0294(5)	0.4093(8)	0.1393(8)	0.018(3)
Zn	Zn7c	4a		0.5319(4)	0.0931(8)	−0.1424(8)	0.011(2)
Zn	Zn7d	4a		−0.5289(4)	−0.0939(8)	0.1435(8)	0.014(2)
Zn	Zn7e	4a		0.6875(2)	0.2546(10)	−0.1451(4)	0.0108(14)
Zn	Zn7f	4a		0.1891(2)	0.7503(10)	−0.1443(4)	0.0078(13)
Zn	Zn8a	4a		−0.0442(5)	0.3615(7)	−0.0488(6)	0.015(2)
Zn	Zn8b	4a		0.0478(5)	−0.3490(7)	0.0534(7)	0.015(2)
Zn	Zn8c	4a		0.4486(5)	0.8474(8)	−0.0518(7)	0.014(3)
Zn	Zn8d	4a		−0.4507(5)	−0.8492(8)	0.0503(7)	0.012(2)
Zn	Zn8e	4a		0.3450(2)	−0.2493(9)	−0.0496(4)	0.0037(12)
Zn	Zn8f	4a		0.8582(2)	0.251(1)	−0.0560(4)	0.0107(13)
Zn	Zn9a	4a		−0.1308(4)	0.0983(8)	−0.1585(8)	0.009(2)
Zn	Zn9b	4a		0.1308(5)	−0.0972(8)	0.1576(8)	0.011(2)
Zn	Zn9c	4a		0.3703(4)	0.6042(7)	−0.1588(7)	0.005(2)
Zn	Zn9d	4a		−0.3675(4)	−0.6087(7)	0.1591(7)	0.009(2)
Zn	Zn9e	4a		0.5126(2)	−0.2482(9)	−0.1585(4)	0.0081(14)
Zn	Zn9f	4a		0.0210(2)	0.2531(10)	−0.1565(4)	0.0111(14)
Zn	Zn10a	4a		0.1141(5)	−0.1517(9)	−0.2502(8)	0.009(3)
Zn	Zn10b	4a		−0.1139(6)	0.1563(9)	0.2491(8)	0.012(3)
Zn	Zn10c	4a		0.4817(2)	0.7497(11)	0.2499(3)	0.0044(14)
Zn	Zn11	4a		0.2491(4)	0.2529(12)	−0.2488(5)	0.037(2)
Zn	Zn12a	4a		0.5017(6)	0.0019(10)	0.0031(10)	0.0212(13)
Zn	Zn12b	4a		0.2423(2)	0.7428(9)	0.0151(4)	0.0232(17)
Zn	Zn13a	4a	0.287(4)	0.7453(9)	0.754(3)	0.0882(11)	0.014(2)
Zn	Zn13b	4a	0.287(4)	0.2546(9)	0.255(3)	0.0926(11)	0.014(2)
Zn	Zn14	4a	0.577(13)	0.8685(3)	0.7553(13)	0.0843(4)	0.0042(14)
Zn	Znx1	4a	0.319(13)	−0.9780(6)	−0.5285(12)	−0.0178(11)	0.0042(14)
Zn	Znx2	4a	0.359(18)	−0.9115(7)	−0.6259(12)	−0.1120(11)	0.0042(14)
Zn	Znx3	4a	0.365(18)	0.9548(7)	0.5672(13)	0.0685(12)	0.0042(14)

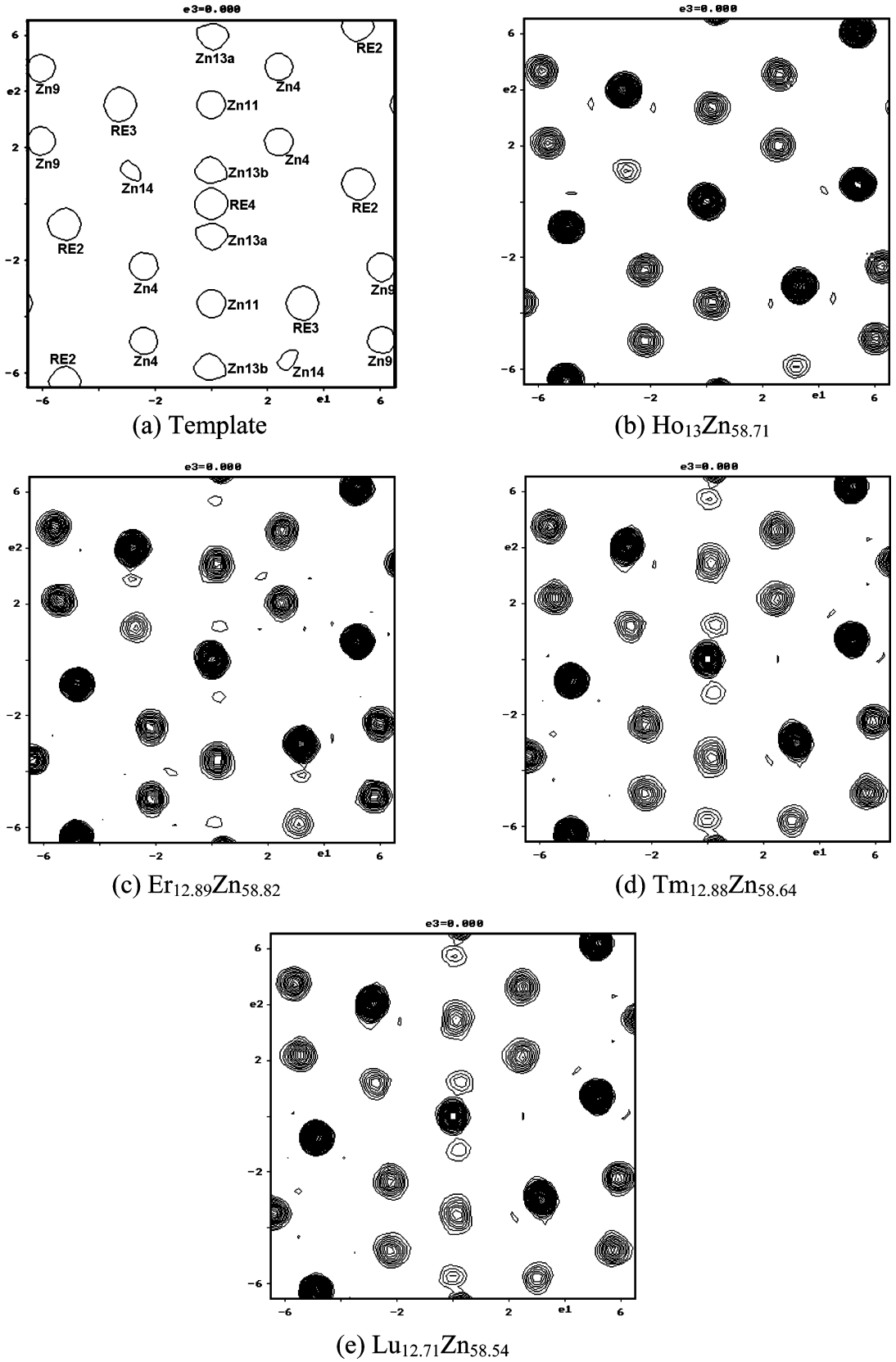

Figure 1. Electron density maps (calculated from F_{obs}) showing the disorder mechanisms I and II. The occupancy of the atom Zn13 (Zn_2 dumbbell) gradually increases as the size of the rare earth decreases from Ho to Lu; consequently, the shape of the electron density corresponding to the position Zn11 atom changes from circular for the Ho case, where Zn13 atom is missing, to pronouncedly elliptic for the Lu case, where the Zn13 atom has the highest occupation. The capping atom Zn14 causing disorder mechanism II is seen to have a similar effect on *RE*3.

correction, based on a shape obtained by optimizing the equivalence for symmetry-related reflection, was performed with the programs *X-RED*[27] and *X-SHAPE*.[28] The refinements of the structures were performed using the program *JANA2000*.[29] The structural analysis

Table 8. Partially Occupied Positions in the $RE_{13}Zn_{58+\delta}$ Compounds

		compound			
		$Ho_{13}Zn_{58.71}$	$Er_{12.89}Zn_{58.82}$	$Tm_{12.88}Zn_{58.64}$	$Lu_{12.71}Zn_{58.54}$
refined occupancy of the Zn pair in the hexad tunnel			0.113(4)	0.120(4)	0.287(4)
refined occupancy of the extra capping atom Zn14		0.378(16)	0.606(14)	0.637(11)	0.577(13)
refined occupancy of the Zn atoms along the sinusoidal chain	Zn1k		0.620(27)	0.710(22)	0.730(25)
	Zn1l	0.5	0.650(27)	0.384(17)	0.600(25)
	ZnX1	0.184(6)	0.386(16)	0.175(11)	0.319(13)
	ZnX2	0.306(7)	0.440(23)	0.620(24)	0.359(18)
	ZnX3	0.213(9)	0.443(15)	0.210(13)	0.365(18)
	ZnX4	0.283(9)	0.220(22)	0.291(16)	
	ZnX5	0.183(8)	0.218(17)	0.366(13)	

electron-density isosurfaces were generated using the program *JMAP3D*.[30] The images were rendered using the programs *DIAMOND*, version 2.1c,[31] and *TRUESPACE*, version 5.2.[32]

A detailed description of the crystal data, data acquisition, and refinements is given in Table 3.

Basic Structural Considerations

In the literature, all of the compounds concerned were assigned the same space group, $P6_3/mmc$ or its noncentrosymmetric counterpart $P6_3mc$.[3] This is most probably due to the work being done using the powder method as a means of structural characterization. Superstructure reflections are then easily missed because of the weakness of their intensities. In the present study, the power of single-crystal X-ray diffraction becomes apparent, and superstructure ordering was detected for all compounds.

The $RE_{13}Zn_{58+\delta}$ compounds formed by the larger elements in the series (Ce, Pr, Nd, Sm, Gd, Tb, and Dy) crystallize in the hexagonal system. Two different disorder mechanisms, I, entailing the exchange of some of the rare-earth content on the hexad (Wyckoff position 2a) by a Zn_2 dumbbell (labeled Zn13a and Zn13b), and II, involving the insertion of an extra atom in the structure (labeled Zn14), were observed[23] and resulted in nonstoichiometry and lowering of the symmetry.

Generally, the reciprocal lattices of all of the compounds in this study are characterized by a doubling of the hexagonal *a* and *b* axes, but the intensity distribution indicates twinning. Further, there are no superstructure reflections in the hexagonal *hk*0 plane, indicating an *n* glide perpendicular to *c** that is forbidden in hexagonal symmetry but allowed in orthorhombic twins. The superstructure reflections simply correspond to a violation of the C-centering of the orthohexagonal setting of the basic unit cell. The Ho-containing compound crystallizes in space group *Pcmn* (*Pnma*), while the remaining three compounds crystallize in $Pc2_1n$ ($Pna2_1$).

The group−subgroup relations are simply

$$P6_3/mmc \xrightarrow{\tau 3} Cmcm \xrightarrow{\kappa 2} Pcmn \xrightarrow{\tau 2} Pc2_1n$$

It is notable that the Ho compound is refinable in the centrosymmetric space group *Pcmn*, while the immediately preceding, lighter, hexagonal congeners crystallize in the noncentrosymmetric group $P6_3mc$. This anomaly is quite easily understood. In the hexagonal structure, the center of symmetry is violated by the presence of the interstitial Zn atom, Zn14, that displaces the neighboring *RE*3 positions away from the mirror plane perpendicular to the hexad. In orthorhombic structures, the mechanism is the same, and the mirror symmetry is indeed violated. However, the enlarged unit cell allows for the presence of an *n* glide that supplants the mirror symmetry. This *n* glide is indeed present in the orthohexagonal setting of the centrosymmetric space group $P6_3/mmc$ (*Cmcm*), where the mirror plane perpendicular to the *c* axis generates an *n* glide in conjunction with the C-centering. In the diffraction patterns of the Ho, Er, Tm, and Lu compounds, the characteristic extinction conditions for the *n* glide were observable only for the Ho compound, and this was refined in the centrosymmetric space group *Pcmn*. As a result of this, the refinement of the Ho compound was rather more stable than that of the other compounds and, in contrast to these, allowed for anisotropic treatment of all atoms. The $Er_{13}Zn_{58+\delta}$ compound was refined using anisotropy for the Er atoms, $Tm_{13}Zn_{58+\delta}$ was refined using anisotropy for most Tm atoms, and $Lu_{13}Zn_{58+\delta}$ was refined with all atoms described isotropically.

The structures of these four compounds are much more complex than those for their counterparts with the early lanthanides,[23] and a new disorder mechanism comes into play.

All structures were solved starting from a model generated from the archetype structure $Ce_{13}Zn_{58}$ in the orthorhombic setting. Pseudomerohedral twinning, due to the broken hexagonal symmetry, was obvious from the diffraction patterns, and this was necessary to model early in the refinement. The volume ratios were refined simultaneously with the relaxation away from metrically hexagonal positional parameters. For the noncentrosymmetric cases, the addition of new twin laws related to the center of symmetry did not yield any improvement. Disorder caused by inter-

(27) Computer code *X-RED*, version 1.07; Stoe and Cie GmbH: Darmstadt, Germany, 1996.
(28) Computer code *X-SHAPE*, version 1.01; Stoe and Cie GmbH: Darmstadt, Germany, 1996.
(29) Petříček, V.; Dusek, M. Computer code *JANA2000*; Institute of Physics AVCR: Praha, Czech Republic, 2005.
(30) Weber, S. Computer code *JMAP3D*; NIRIM: Tsukuba, Japan, 1999.
(31) Brandenburg, K. Computer code *DIAMOND*, version 2.1c; Crystal Impact: Bonn, Germany, 1999.
(32) Ormandy, R. Computer code *TRUESPACE*, version 5.2; Caligari Corp.: Mountain View, CA, 2000.

Electron density map of complete model

Residual density from a model without ZnX atoms

Structural drawing of complete model

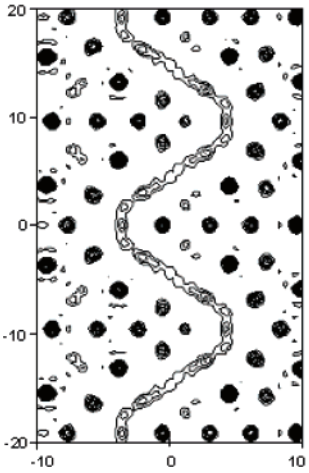

(aI) $Ho_{13}Zn_{58.71}$

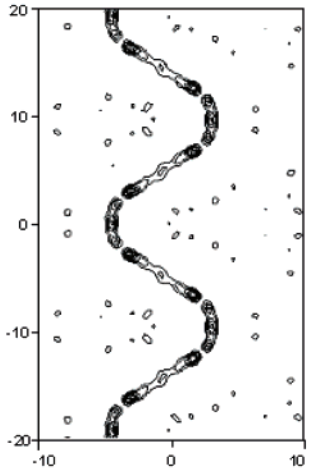

(aII) $Ho_{13}Zn_{58.71}$

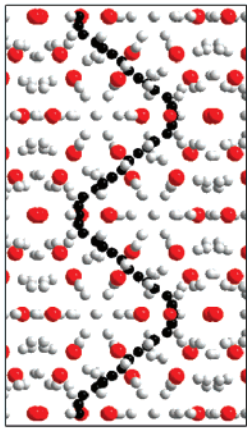

(aIII) $Ho_{13}Zn_{58.71}$

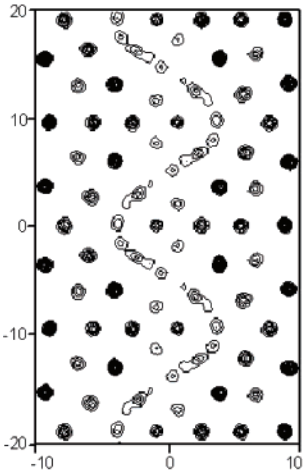

(bI) $Er_{12.89}Zn_{58.82}$

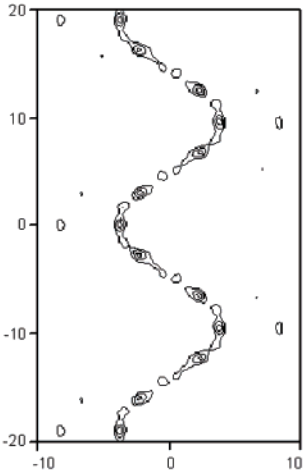

(bII) $Er_{12.89}Zn_{58.82}$

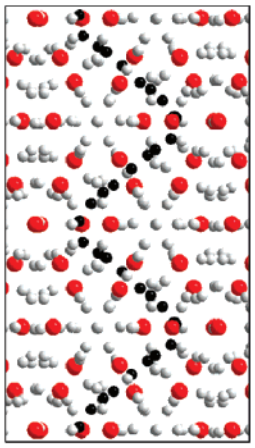

(bIII) $Er_{12.89}Zn_{58.82}$

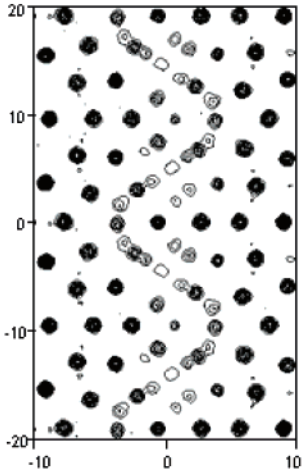

(cI) $Tm_{12.88}Zn_{58.64}$

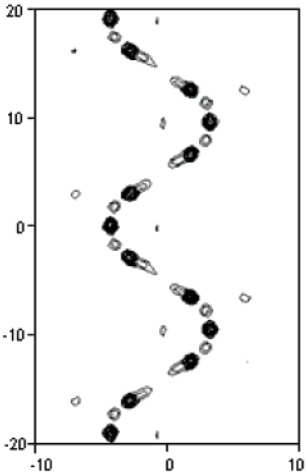

(cII) $Tm_{12.88}Zn_{58.64}$

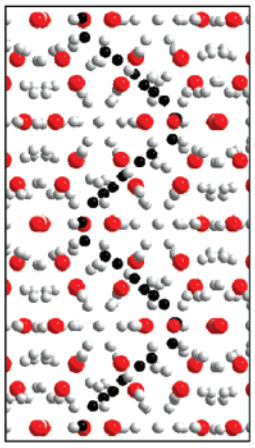

(cIII) $Tm_{12.88}Zn_{58.64}$

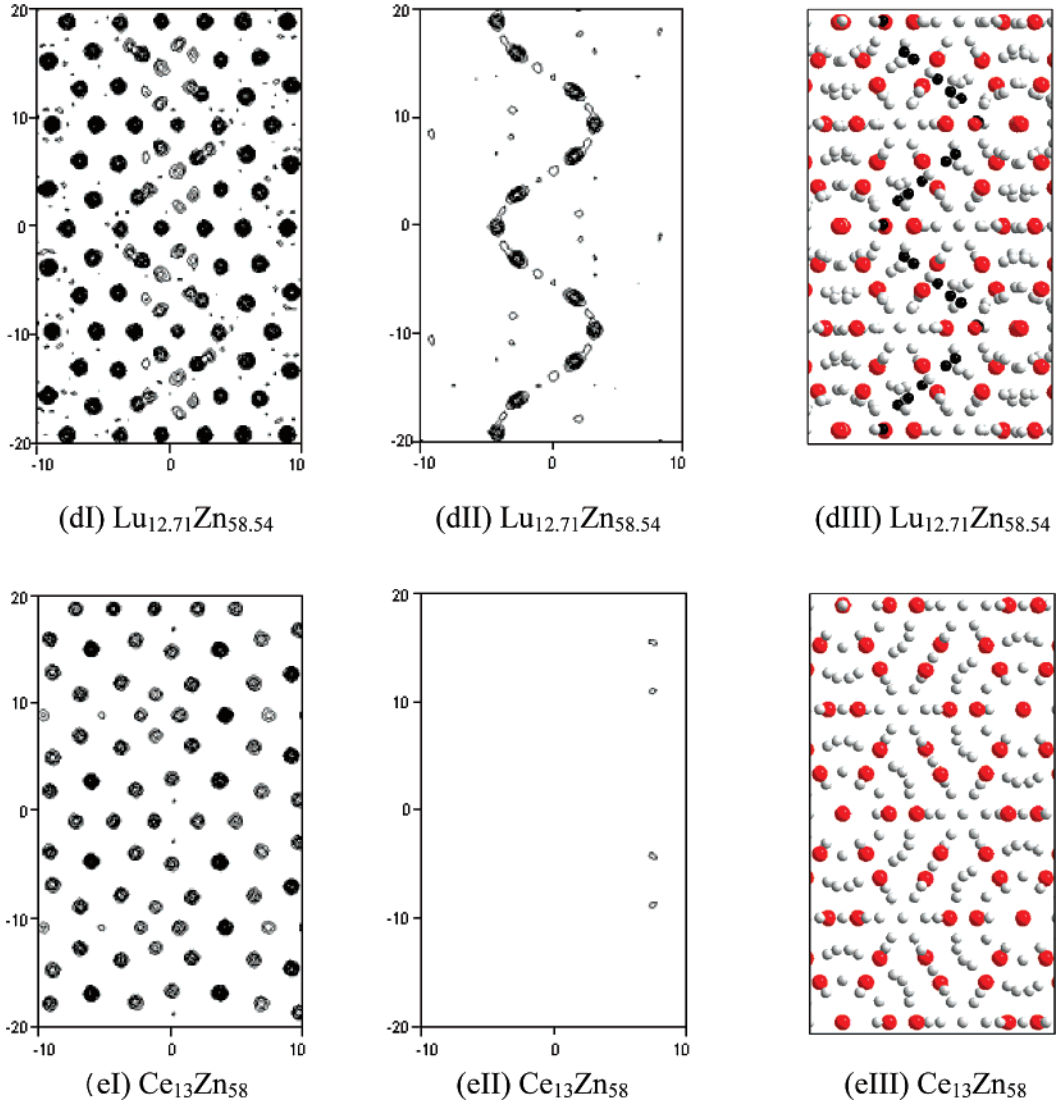

Figure 2. Parts aI−eI, aII−eII, and aIII−eIII represent the electron density maps, difference electron density maps, and structures for the $Ho_{13}Zn_{58.71}$, $Er_{12.89}Zn_{58.82}$, $Tm_{12.88}Zn_{58.64}$, $Lu_{12.71}Zn_{58.54}$, and $Ce_{13}Zn_{58}$ compounds, respectively. The horizontal direction is [−101], and the vertical direction is [010]. Tick marks are set each 10 Å. The larger spheres in red are *RE* atoms, and the smaller spheres are fully occupied Zn atoms (in light gray) and partially occupied Zn atoms (in black). The partially occupied Zn atoms permeate the structure along the orthorhombic *b* direction and result in disorder mechanism III in the Ho, Er, Tm, and Lu compounds, while there is no such phenomenon in the Ce compound.

stitials was recognized from residual electron densities and refined. Partially occupied positions were refined using a common isotropic displacement parameter to make the comparison between occupations meaningful. The addition of new interstitial positions was ceased when their refined occupancy converged to a value of less than 10%. This value is quite arbitrary, but it was clear from the refinements that inclusion of such minor contributors to the scattering did not alter the quality of the refinement greatly, neither in terms of agreement (*R* values) nor in terms of residual electron densities. For the two atoms making up the Zn_2 dumbbell (Zn13a and Zn13b) that partially replaces *RE*4, occupancy was assumed to be identical, and the occupancy sum Zn13a + *RE*4 was set to unity. In the Lu structure, there is a relative paucity of interstitial positions. This may reflect the fact that space in this structure is more limited and that this precludes the more liberal sprinkling of interstitial positions along the sinusoidal locus visible for the other cases.

Structural Description and Discussion

For ease of comparison, atomic labels used in the hexagonal structures were maintained as far as possible for describing the corresponding atomic positions in the orthorhombic structures.

The fundamental building block for the orthorhombic structures is the same as that for the hexagonal structures: a double-pentagonal antiprism. The hexagonal 13:58 structures contain four independent *RE* atoms (*RE*1 and *RE*3 in Wyckoff position 6h, *RE*2 in 12k, and *RE*4 in 2a), while Zn occupies 14 independent positions.[23] In addition to the positions in the hexagonal structures, several partially occupied Zn positions, ZnX1, ZnX2, ZnX3, ZnX4, and ZnX5, were introduced in the orthorhombic structures. The atomic positions, isotropic temperature parameters, and occupancies (when applicable) are given in Tables 4−7.

To inspect whether disorder mechanisms I and II occur in the orthorhombic system, it is instructive to draw the 13

Å × 13 Å section of the electron density of the structures, as was previously done for the hexagonal system.[23] This section is defined by the $\langle 100 \rangle_{hex}$ and $\langle 001 \rangle_{hex}$ directions and contains the origin (compare Figure 1a−e).

In the Ho compound (Figure 1b), no Zn_2 dumbbell (atomic positions Zn13a and Zn13b) appears in the electron density map, but an interstitial atom that corresponds to the position of Zn14 is clearly evident, indicating the existence of disorder mechanism II but not disorder mechanism I. In fact, the Ho compound is the only compound in which disorder mechanism II has been observed independently from mechanism I. For the Er−Lu compounds, the Zn14 atoms can be clearly seen in the electron density map (at a contour value of 7 e $Å^{-3}$), indicating the occurrence of disorder mechanism II. The Zn_2 dumbbell is evident in the electron density map (Figure 1c−e), and the density of the dumbbell atoms is even more pronounced for the Lu compound (Figure 1e). Thus, both disorder mechanisms I and II come into play for the Er, Tm, and Lu compounds. The relationship between the occupancy of the Zn_2 dumbbell and the size of the *RE* atoms is apparent from Table 8.

In the hexagonal system, disorder mechanisms I and II are active. However, for the orthorhombic system, yet another disorder mechanism kicks in; a sine-wave-like electron density permeates the structure along the orthorhombic *b* direction in all of the title compounds, disorder mechanism III. This disorder mechanism is clearly visible in the electron density maps (compare Figure 2aI−dI) and difference electron density maps (Figure 2 aII−dII) generated from the model without interstitial Zn. The similarity between F_{obs} of the models containing interstitial Zn and $F_{obs} - F_{calc}$ for models devoid of interstitial Zn is a strong indication that the modeling of interstitials is robust. In the structures crystallizing in the hexagonal system, there is no indication of such a disorder mechanism. As a reference, the same section of the electron density map for the Ce compound is shown in parts eI and eII of Figure 2. Parts aIII−dIII of Figure 2 show the structures of the orthorhombic compounds. The sine-wave-like behavior is clearly seen and may be compared to the simpler structure of the Ce compound in the orthorhombic setting (Figure 2eIII).

The atomic positions used to model the sine-wave-like electron densities form a chain of partially occupied orbits, where simultaneous occupancy of neighboring sites is impossible because of the short mutual distances.

Figure 3a represents the electron density isosurface of the sine-wave-like chain at the 7 e $Å^{-3}$ level generated from F_{obs} data. Because the atomic positions on the chain cannot be described accurately, there are many possibilities for the arrangement of coordination polyhedra. We must assume local ordering propagating through the crystal, and this leads to the formation of rather different local environments. Figure 3b illustrates a model for the arrangement of the atomic positions on the chain; the Zn atoms in green form one set that may all be present simultaneously, and the Zn atoms in orange present another possibility. The atoms in yellow are the centers of the cubes and coexist with the green ones. Figure 3c shows the effect of the green set of Zn atoms on the local coordination environment, while Figure 3d shows the corresponding pattern for the orange set. Note how the partially occupied positions for Zn lead to new coordination polyhedra for the *RE* atoms. The presence of capping atoms on both pentagonal faces of the $RE Zn_{15}$ double-pentagonal antiprism leads to a $RE Zn_{17}$ polyhedron, and the capping of one face by two Zn atoms leads to the formation of a $RE Zn_{18}$ polyhedron.

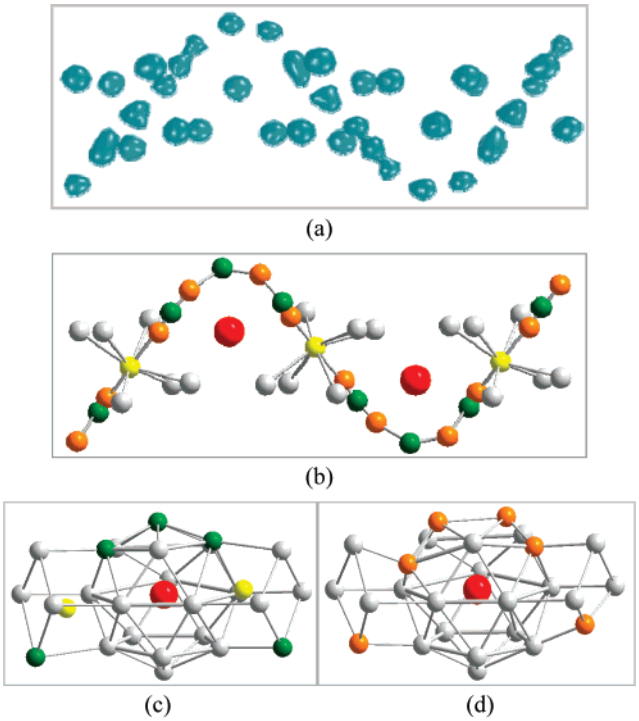

Figure 3. (a) Electron density isosurface of the sine-wave-like chain at contour 7 e $Å^{-3}$ generated from F_{obs} data for the $Er_{12.89}Zn_{58.82}$ compound. (b) Self-consistent model for the arrangement of the atomic positions on the chain. The larger red spheres are the Er atoms, and smaller gray spheres are the fully occupied Zn atoms. The rest are the partially occupied Zn atoms. In part c, the green set of Zn atoms of the local coordination environment form a $RE Zn_{17}$ polyhedron and occupancy of the centers of the neighboring cubes is allowed (yellow). In the corresponding pattern for the orange set, a $RE Zn_{18}$ polyhedron is formed (d). This probably leads to vacant neighboring cubic interstices.

The cubic interstices notable in the cubic 1:1 approximants[20,22] are found also in the orthorhombic systems, and it may be noted that the propagation of partially occupied positions makes it probable that cubic interstices of neighboring $RE Zn_{17}$ polyhedra should be centered by Zn while that next to a $RE Zn_{18}$ polyhedron would probably be vacant. The distortion of the shape of the cubic interstices also indicates that this should be the case.

The structures of the orthorhombic compounds are found to be related to the $RE Cd_6$ phases by a common structural motif, which differs only in the arrangement of some *RE*Zn polyhedra and in the capping of some of their pentagonal faces. The difference between the building unit of $RE_{13}Zn_{\sim 58}$ and that of the $RE Cd_6$ phases is that in the $RE Cd_6$ compounds there exists only a monocapped, double-pentagonal antiprism ($RE Zn_{16}$ polyhehedra; Figure 4a), but in the $RE_{13}Zn_{58+\delta}$ phase additionally there exist uncapped, double-pentagonal antiprisms ($RE Zn_{15}$ polyhedra; Figure 4b) and double-capped

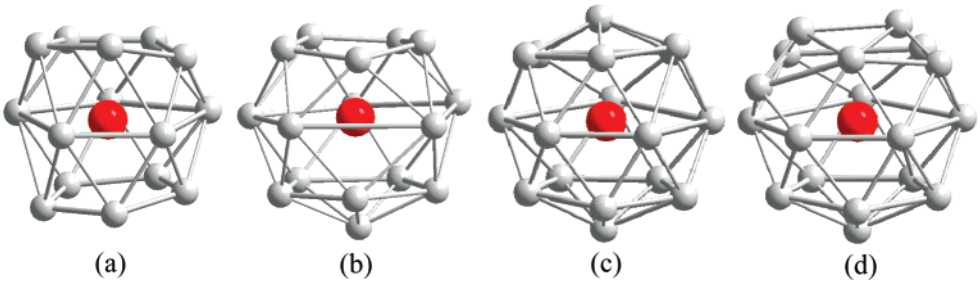

Figure 4. Types of $RE\text{Zn}_x$ polyhedra appearing in the orthorhombic structures: (a) $RE\text{Zn}_{15}$; (b) $RE\text{Zn}_{16}$; (c) $RE\text{Zn}_{17}$; (d) $RE\text{Zn}_{18}$.

antiprisms [$RE\text{Zn}_{17}$ polyhedra (Figure 4c) and $RE\text{Zn}_{18}$ polyhedra (Figure 4d)].

There is no simple trend for the Zn content in these compounds. For the early hexagonal members of the sequence, the decrease in the atomic radii of the rare-earth elements is matched by a decrease in the unit cell volumes. When disorder mechanism I becomes active, the Zn content increases, and the shrinkage in the unit cell volume becomes less apparent. The effect is, however, expected to be small because the addition of the Zn_2 dumbbells is made at the expense of the occupancy of the rare earth in Wyckoff position 2a. As disorder mechanism II becomes active, the volumetric shrinkage becomes even less pronounced, and the unit cell content peaks for the fully ordered Tb compound $Tb_{13}Zn_{59}$. In this structure, the size of the rare-earth atom is sufficiently small to allow for the full occupancy of the extra Zn atom Zn14, while the Zn partial structure is still open enough to allow for full occupancy of the cubic interstices. As the sizes of the rare-earth atoms progress to even smaller values, the cubic interstices shrink and can no longer hold interstitial Zn, unless the surrounding structure allows for some flexibility. The cubes tend to deform rhombohedrally, in complete analogy to the closely related cubic compounds.[22] As the filled cubes deform, their vertices come into close contact with the position Zn14 and a complicated ordering/disordering takes place. Cube centers, cube vertices, and the Zn14 position come too close for simultaneous occupation, and they all become partially occupied. Large thermal parameters signal strong local coupling between these positions. As the unit cell shrinks, the Zn content goes down, and for the Lu compound, the stoichiometry is back close to $Lu_{13}Zn_{58}$. It may be inferred that the increase in the Zn content noted in the early part of this structural sequence can be attributed to free space becoming available in the immediate vicinity to the rare-earth atoms. The surrounding Zn network responds relatively weakly to the decrease in the rare-earth volume. After the peak value is reached for the compound $Tb_{13}Zn_{59}$, Zn−Zn repulsion becomes dominant. A further decrease in the cell volume now leads to a decrease in the Zn content from disorder mechanism III. Note, however, that disorder mechanism I again becomes more pronounced as the rare-earth size decreases from Ho to Lu. It would appear that the local environment here is less susceptible to the general shrinkage, and thus the reduction of the rare-earth size leads to increased room for Zn.

It should be noted that this discussion is a simplification of the behavior of the system. Most of the compounds are expected to have a certain homogeneity range, and for Tb, two different compounds have been isolated, having rather different compositions and structures,[23] while for Ho, the sample was found to order incommensurably for one synthesis.[24] Local ordering is thus a product not only of geometrical factors but also of equilibrium conditions such as the composition in the melt and temperature of formation.

Conclusions

The formerly assigned prototype structures of the $RE_{13}Zn_{58}$ phases have been proven to be insufficient for a full description. An additional disorder mechanism (III) comes into play in the orthorhombic system for Ho-, Er-, Tm-, and Lu-containing compounds. A remarkable difference between the orthorhombic system and the hexagonal system is that a further ordering of the metal vacancies in some of the cubic interstices caused by the disorder mechanism III is prominent in these structures.

The intricate interplay between the $RE-Zn_2$ pair exchange and the vacancies in the cubes, combined with the occasional formation of $RE\text{Zn}_{17}$ and $RE\text{Zn}_{18}$ polyhedra by the presence of one or two additional Zn atoms, causes the nonstoichiometry of the compounds. For the Ho compound, we reported earlier[24] on an incommensurate ordering mode. It is interesting that the occurrence of such an extra ordering seems to be dependent on subtle compositional differences or, possibly, on the thermal history of the sample. For the other compounds covered in this study, we found no evidence of incoherent ordering, neither as weak satellite reflections nor as diffuse scattering. There is no conclusive evidence that local ordering does not exist. Indeed, we firmly believe that local ordering is essential to understanding the localized positions on the sine-wave-like occupancy wave, but apparently the coherence length is too short for this order to leave any detectable fingerprint in the diffraction pattern. A more detailed study varying the temperature and composition may reveal such behavior.

Acknowledgment. Financial support from the Swedish Natural Science Research Council and the Foundation for Strategic Research is gratefully acknowledged.

Supporting Information Available: The CIF files for the four compounds. This material is available free of charge via the Internet at http://pubs.acs.org.

IC700476W